Localized crystallization of Germanium nanowires

– Laboratory of Semiconductor Materials –

Travaux pratiques IVa, Physics Master

submitted by

Daniele Cucurachi

January, 2021

Daniele Cucurachi
daniele.cucurachi@epfl.ch
Student ID: 328929

Supervisors

1st: Dr. Santhanu Panikar Ramanandan
2nd: Prof. Anna Fontcuberta i Morral

École polytechnique fédérale de Lausanne (EPFL)

Contents

1 Motivations

This work aims to investigate which are the best rapid thermal annealing (RTA) parameters for crystallizing Germanium nanowires grown on a patterned Silicon substrate, with the prospect of employing the nanowires as quantum dots for quantum computing applications (hole spin qubits). To this purpose, the features we are looking for are good quality and defects free crystal structure and epitaxy with Silicon. Indeed, the presence of an epitaxial relation between Germanium and Silicon will lead to a hole mobility enhancement. There is a lattice mismatch of 4,2% between Si and Ge (since Ge has a greater lattice parameter with respect to Si) which induces a compressive strain in the Ge crystal structure when it is epitaxially grown on Si at room temperature. On the other hand, Ge features a larger thermal expansion coefficient so, after the annealing process (temperatures higher than 500°C), a reverse situation occurs: Ge undergoes tensile strain because it shrinks more when cooled down after annealing. The induced strain lifts valence band degeneracy (heavy hole and light hole bands are degenerate at gamma point in Germanium) reducing interband scattering with a consequent hole mobility enhancement. Ge nanowires could also relax this strain by forming misfit dislocations at the interfaces between the two materials. In this case we would lose the mobility enhancement effect induced by strain, thus we want to avoid the formation of defects at the interface. We also want to avoid the presence of Si intermixing, which could be induced by high temperature annealing, since it would be detrimental for quantum dots.

Ordered array of nanowires have been fabricated on an e-beam patterned Si substrate by evaporation using the lift-off technique. They were successively crystallized, using the solid phase epitaxy approach (SPE), by rapid thermal annealing. This unconventional approach has been chosen because of the scalability: the possibility of mass production is fundamental since a large number of semiconductor qubits are required for quantum computing applications. In addition, evaporation allows to grow nanowires networks. This is extremely useful for quantum computing since it provides a simple way to link different quantum dots obtaining qubits superposition. The nanowires have been then analyzed through Raman spectroscopy, scanning and transmission electron microscopy.

2 Introduction

In the following section I will present a brief overview on Germanium nanowires and related fields of application (subsection 2.1), with a special focus on hole spin qubits (subsection 2.2).

2.1 Germanium nanowires

During the second half of 20th century, Germanium, largely used in semiconductor industry, was replaced by Silicon due to the better structural and electrical properties of the Si/SiO_2 interface. Indeed, Si exhibits superior oxide properties with respect to GeO_2 (which is soluble in water and lacks stability) and higher operational temperature limit.
Germanium is nowadays captivating more interest in various fields thanks to his peculiar properties: Germanium has a smaller effective mass and an higher carrier mobility compared with Silicon (electron mobility is around $3900cm^2/(Vs)$ and hole mobility $1900cm^2/(Vs)$ [1]). It can be epitaxially grown on Si wafers, guaranteeing integration with current Silicon technology in modern semiconductor industry. In addition, Ge is a suitable material for investigating quantum size effects thanks to to his large Bohr exciton radius [2].

Ge can be used to produce nanowires (NWs), one-dimensional nanostructures characterized by a high surface to volume ratio which leads to unique physical properties, different from bulk material's ones. Ge nanowires in particular, thanks to the easy synthesis process and the high carrier mobility (on the order of $600cm^2/(Vs)$ for holes [3]), are captivating much interest as promising technology for high performance electronic devices [4]. Moreover, strain engineering allows to further improve nanowires properties, in particular hole mobility (section 1 for more details).
Both Germanium and Silicon, in their bulk crystalline form, exhibit an indirect bandgap, indeed conduction band minimum is respectively located at the L and X-point, the valence band maximum instead at the center of the Brillouin zone. In this case, phonons are involved in radiative recombination and absorption processes in order to preserve momentum, leading to poor light emission and absorption properties. On the other hand, multiple investigations showed that hexagonal crystal phase Ge, Si or Si_xGe_{1-x} compounds reveal direct band gaps [5, 6], paving the way for possible applications in optoelectronics [7]. Indeed, semiconductors grown in the form of nanowires can exist in various crystal phases, some of them not achievable in bulk material. This phenomenon is called polytypism [8].
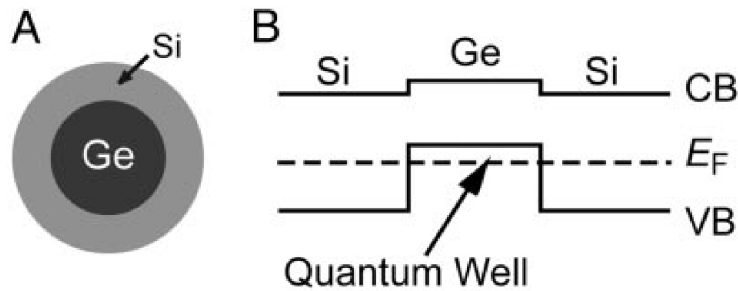Despite recent progresses, Ge remains much less explored and understood than Si.

2.2 Hole Spin Qubits

Ge nanowires can be exploited also for quantum computing applications. The purpose for the next step of this project is, indeed, fabricating Ge-Si core-shell quantum dots to implement hole spins qubits [9, 10]: Ge is a promising material for electrically tunable hole spin qubits thanks to the strong and tunable spin-orbit coupling that allows rapid control of single spins.

Since semiconductor qubits feature an extremely low coherence time, quantum computing devices exploiting semiconductor qubits require a large number of qubits so that quantum error correction can be properly applied. This is why we adopted e-beam evaporation and lift-off, which is a scalable approach.

In order to fabricate quantum dots a pure Si shell is deposited on the Ge nanowires. Between Ge and Si there is a valence band offset of 0,5 eV which is exploited in Ge-Si core-shell NWs in order to accumulate holes in the Ge core, provided that the Fermi level lies below Ge valence band maximum (see Figure 1). This energy offset at the interface acts as a potential barrier that confine holes in the Ge channel. In Ge-Si core-shell NWs hole mobility can be enhanced by lifting the light and heavy hole band degeneracy through strain engineering (section 1 for more details) and has been reported the observation of ballistic transport on lengths up to the order of hundreds of nanometers [9]. Quantum dots for quantum computing applications can be obtained by placing contacts on the core-shell nanowires and isolating a single hole spin. Usually, a Schottky barrier forms at a metal-semiconductor junction since semiconductor Fermi level lies inside the band gap, but in Ge-Si NWs the Fermi level lies below Ge valence band edge allowing to have reproducible transparent contacts through annealing.

Source: [9]

Figure 1: *Si-Ge core-shell nanowire cross-section (left) and the corrisponding band diagram (right)*

3

3   Analysis Techniques

In the subsequent section I will present the analysis techniques employed in the present work: Raman Spectroscopy (subsection 3.1), Scanning and Transmission Electron Microscopy (subsection 3.2). For each of the analysis techniques, after a brief general introduction, I will report the specifications we adopted and important remarks and observations related to the project.

3.1   Raman Spectroscopy and Ge dispersion relation

Raman Effect

Raman effect consists in anelastic scattering of electromagnetic radiation on a crystal resulting in frequency shift of diffused radiation. Photon scattering can be elastic (Rayleigh scattering), if no phonons are involved in the process, or anelastic, if one or more (high order Raman scattering) phonons are involved. Since the phenomenon undergoes energy and momentum conservation laws, diffused photons feature a different energy with respect to incident ones. This frequency shift is a consequence of the creation (Stokes) or annihilation (anti-Stokes) of one or more phonons.

It is a weak effect but can be enhanced in back scattering configuration, i.e. with the radiation hitting perpendicularly the material, or by other means like SERS effect (Surface Enhanced Raman Scattering) which is a technique that maximize Raman scattering by means of nanostructures or molecules adsorbed on the material surface [11].

Raman spectroscopy

Raman spectroscopy is a versatile nondestructive spectroscopy technique which exploits Raman effect. After the sample is hit by a monochromatic radiation, the signal intensity of inelastically diffused photons is detected in order to analyze the energy shift.

It is used for various kind of analysis: identification of vibrational and rotational modes, crystal quality and crystal phase analysis, defect and stress assessment, compositional analysis. It can be used also to probe the electronic band structure and the electron-phonon interaction in semiconductors.

For our analysis we used two different Raman spectrometers: the material science department Raman spectrometer and the Renishaw confocal Raman spectrometer in physics department. The material science department Raman spectrometer is characterized by a higher resolution, which is about 0.2 cm^{-1}, but requires more time for the measurement process with respect to the Renishaw spectrometer. It is equipped with two lasers, blue (488 nm) and green (532 nm), whose laser spots have a diameter of about 2 um (value provided by Elias Stutz). This is a crucial

aspect to consider, since the nanowires have widths on the order of hundreds of nm the laser will mostly hit the substrate during a measurement, thus the CCD will detect a strong signal from Silicon. Si background signal subtraction will be fundamental for our analysis (see Figure 9 for more details on the Si baseline subtraction method). The Raman spectrometer was used in additive mode (18-18-18): the radiation diffused by the sample is diffracted three times by three diffraction gratings (the numbers 18-18-18 are related to the diffraction gratings angles) before hitting the CCD, at each reflection the frequency range we are interested in is selected by a slit.

On the other hand, the Renishaw confocal Raman spectrometer shows a more compact set up and is characterized by a resolution of 0.8 cm^{-1} and a faster measurement process. It is equipped with an integrated optical microscope and various lasers: 405 nm, 488 nm, 532 nm and 785 nm, which have a spot size of about 1 um.

For the measurements we chose to use 532 nm laser for two reason: we wanted to compare results from the two instruments, so we selected a laser common to both the spectrometers, and we needed to choose a laser powerful enough to excite Ge optical phonons. Fukata et al. estimated the penetration depth of 532 nm laser in Ge nanowires to be about 20 nm in the nanowires [12].

We used Raman spectroscopy to investigate crystal quality and asses the presence of strain, defects and Si-Ge intermixing.
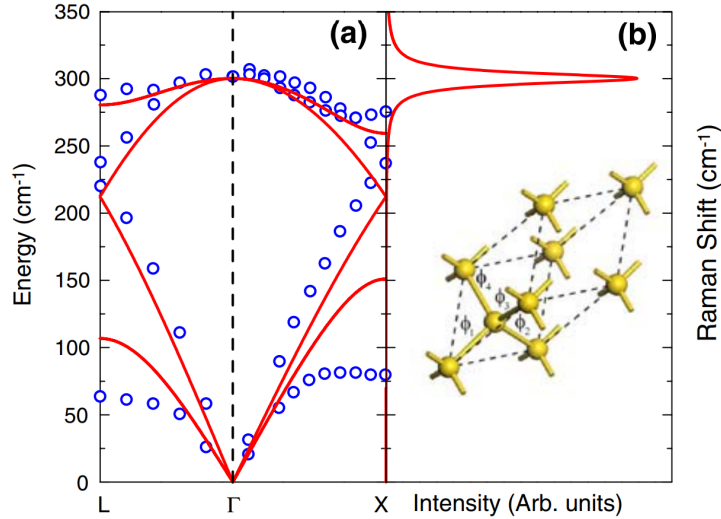
In the following will be presented two fundamental points for interpreting Ge nanowires (on Si substrate) Raman spectra: Ge phonon dispertion relation and the features of a standard Si-Ge Raman spectra.

Germanium phonon dispersion relation

The phonon dispersion relation of Ge nanowires [13, 14], which describes the phonons behavior, is crucial to analyze Ge Raman spectra since Raman spectroscopy relays on photon-phonon interaction. Ge NWs dispersion relation displays two optical phonon branches and two acoustic phonon branches (Figure 2). Raman spectrum of a perfectly crystalline Ge sample exhibits a sharp peak around 300 cm^{-1} [15, 16], which corresponds to the highest frequency of optical modes at the gamma point. Indeed, in the frequency range used in Raman spectroscopy, light cannot provide k to the system since photon wave vector is negligible with respect to the first Brillouin zone size. The phonon-photon interaction process undergoes momentum conservation allowing only the participation of phonon modes around the gamma point (k=0), in particular optical modes since we are considering Raman scattering (the phenomenon involving acoustic phonon modes is called Brillouin scattering). In principle only infinite wavelength modes at the gamma point can be activated in a Raman experiment, thus the selection rule can be visualized as a delta centered in the gamma point. In the real case Germanium optical modes have finite wavelengths meaning that the phonon selection rule can be represented by a sharp gaussian at the gamma point, whose width can be defined in accordance

with Heisenberg uncertainty principle.

However, impurities or defects in the crystal structure can scatter phonons. This can lead to the activation of phonon modes with a wave vector different from zero, which means lower frequencies modes (lower energies), as it can be clearly seen in Figure 2.

Source: [13]

Figure 2: *(a) Ge dispersion relation theoretically calculated (red line) and experimental results (blue circles), by Alfaro-Calderon et al. (b) Ge optical modes Raman peak.*

For these reasons we expected to see only shifts towards lower Raman shift values in our Raman measurements, in case the nanowires exhibit a defective structure. Similar effects on Raman spectra can be induced also by strain: applied strain changes the lattice parameter, increasing or decreasing the first Brillouin zone size with consequent effects on the dispersion relation. Tensile strain will lead to lower energies shift (red shift), while compressive strain will lead to higher energy shift (blue shift). In the present work, we aimed to induce tensile strain through annealing in the nanowires structures in order to enhance hole mobility (section 1 for more details) thus we expected to spot a red shift in the spectra.
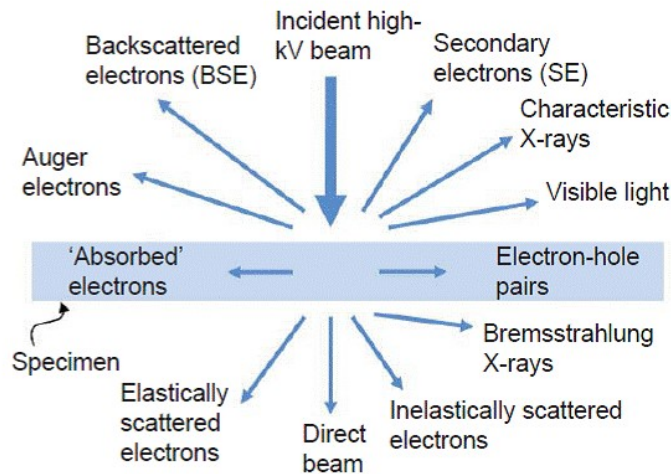
Germanium Raman Spectrum

In order to interpret a Raman spectrum is crucial to know what peaks we should expect from our analysis. In a standard Raman spectrum of Si-Ge compound three peaks are clearly visible: an intense Si-Si peak at 500 cm^{-1}, a Si-Ge peak at 400 cm^{-1} due to interdiffusion (if present) and a Ge-Ge peak at 300 cm^{-1}. There are

also low intensity peaks around 430 cm^{-1} and 480 cm^{-1} due to Si vibrational modes activated by the fluctuation of the number of surrounding Ge atoms [17].

3.2   Scanning and Transmission Electron Microscopy

Scanning electron microscopy and transmission electron microscopy are microscopy techniques that exploit various signals coming from the interaction of an electron beam with the sample in order to produce an image. SEM is one of the most versatile instruments for micro and nanotechnology, characterized by an easy sample preparation and the possibility to perform in-situ experiments. Since electron wavelength is tunable, by means of the accelerating voltage, SEM can reach nanometric resolution breaking diffraction limit of optical microscopy. The resolutive power is not limited by the nature of electrons, as for light in optical microscopy, but by the defects affecting electron lenses, like astigmatism, spherical and chromatic aberrations.

Source: [18]

Figure 3: *Different signals coming from the electron beam interaction with the sample. These signals are exploited in electron microscopy to produce an image of the sample. Each of these signals contains different kind of information.*

Thanks to the various signals resulting from the electron beam interaction, detected by suitable detectors, it is possible to obtain different kind of information about the sample: secondary electrons contain information on topography and morphology, X-rays and Auger electrons on chemical composition, backscattered electrons on elements distribution.

7

TEM exploits different kind of signals: transmitted electrons produce an image of the sample on a camera detector (or a fluorescent screen) while elastically scattered electrons form diffraction patterns which contain information about the crystal structure. Inelastically scattered electrons instead allow chemical analysis, as well as X-rays. It can reach higher resolution with respect to SEM (atomic scale) but requires thin samples in order to obtain an intelligible signal.

For our analysis we used a high-resolution scanning electron microscope (Zeiss Merlin), operating voltage of 2 kV, equipped with an In-Lens (annular) detector, an Energy Selective Backscatter (in-column) detector and a HE-SE2 (Everhart-Thornley) detector. SEM has been used to assess the real size of nanowires and investigate the surface, before and after rapid thermal annealing.

In order to assess the presence of defects and analyze nanowires crystal structure we used a scanning transmission electron microscope (TermoFisher Talos F200S), which also allows to perform energy dispersive X-ray analysis (EDX) for chemical composition. A chemical characterization of the samples through EDX was carried out to investigate the presence of Oxygen at the interface between Si and Ge.

4 NWs Fabrication and Experimental Procedure

In the present section I will briefly present the techniques implemented in the NWs fabrication process (subsection 4.1). I will then describe in details the experimental procedure we followed for the NWs fabrication and for the successive analysis (subsection 4.2). The results of these analysis will be presented in the next section (section 5).

4.1 Fabrication Techniques

This subsection 4.1 provides a concise theoretical background on the techniques implemented in the NWs fabrication process. In case the reader is already familiar with these techniques (e-beam evaporation, lift-off and solid phase epitaxy) it is suggested to skip directly to subsection 4.2, where the NWs fabrication process and the experimental procedure are presented in details.

Electron Beam Evaporation

In the present work e-beam evaporation was employed to deposit Germanium on a patterned Silicon substrate. E-beam evaporation [19] consists in evaporating a target material heating it up by means of an electron beam. The target material, in the form of tablets or grains, is placed in a crucible, then is hit by a highly energetic electron beam. The electron gun is constituted by a Tungsten filament: when it is heated up, Tungsten emits electrons which are accelerated by an applied voltage and precisely focused on the target.
The main advantage of e-beam evaporation is that, thanks to the focused electron beam, contaminations are avoided since the crucible is not heated up during the process.

Lift - Off

After Germanium deposition, the nanowires were obtained by means of the conventional lift off technique. Lift-off technique [20] consists in creating an inverse pattern (the negative of the desired pattern) in a sacrificial resist deposited on a substrate by removing material. The resist is exposed to light (optical lithography) or to an electron beam (e-beam lithography) in order to selectively remove material and create the initial pattern, then is developed in a suitable solvent: in case of positive resist the exposed parts are washed away, in case of negative resist instead the non-exposed parts are washed away. The target material, sputtered or deposited over the all substrate area, can thus reach substrate surface where the resist have been removed. In the end, the resist is washed out by means of a solvent, leaving the target material only where it came in direct contact with the substrate. This reveals the real pattern, which can reach nanometric features.

Solid Phase Epitaxy

In the end, amorphous nanowires were crystallized through rapid thermal annealing using the solid phase epitaxy approach. The Solid phase epitaxy (SPE) approach consists of crystallizing an amorphous material deposited on a crystalline substrate which acts as a template. After the amorphous layer deposition, the crystallization is induced by heating: the material is heated in order to reach the glass transition temperature at which the amorphous phase crystallize by gradually rearranging the atoms, starting from the interface where it can exploit the crystalline substrate as a template. Since the temperatures involved in the process do not reach the material melting point, the crystallization occurs in the solid phase.

4.2 Experimental Procedure

A flow chart representing the NWs fabrication process is depicted in Figure 4. A Silicon wafer (100), p-type, 525 um thick, polished on one side, with a diameter of 100 mm and a resistivity of 0.1 - 0.5 Ohm.cm was used as substrate. Prior to starting the deposition process the substrate was cleaned by oxygen plasma etching (dry etcher Tepla GIGAbatch).
After that, poly methyl methacrylate (PMMA) 495K A4 and methyl methacrylate (MMA) EL6, positive e-beam resists formed by long chain polymers, were separately spin coated on the Silicon substrate in order to obtain two layers with a thickness of 100 nm, with PMMA on top of MMA. The pattern was created through e-beam lithography (Raith EBPG5000+, electron beam lithography system) without mask, relying on a gds file. The exposed resist was successively developed with a solvent, revealing the pattern.
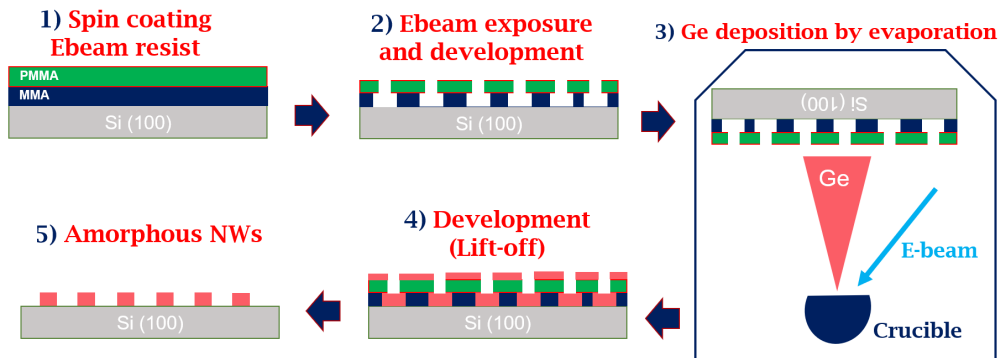

Figure 4: *Schematic representation of the fabrication process: PMMA and MMA were spin coated on the 100 Si substrate, than a pattern was created through e-beam lithography. Successively, Ge was deposited on the patterned Si substrate by means of e-beam evaporation. In the end, the lift-off was completed by removing the resists through a suitable solvent.*

After Silicon wafer cleaving, the native oxide (Silicon Dioxide) was removed by wet etching through a solution containing 1% of Hydrofluoric acid (Acid Bench) and Germanium was deposited on the patterned Si substrate by means of e-beam evaporation (evaporator Leybold optics Lab 600H, Ge 99,99%). The substrate was then soaked in acetone for one night to remove the resists, completing the lift-off procedure.

On a single wafer were realized 25 chips, within these chips were grown different kind of nanowires with varying width, length ,orientation, pitch and arrangements (images (a,b,d) in Figure 5):

- Length: 1um, 5um, 10um, 25um, 50um

- Width: 45nm, 65nm, 95nm, 135nm

- Height: 20 nm (for all the NWs)

- Orientation: 100, 010, 110

- Pitch: 1um, 3um, 5um

In addition, also various nanowires networks were produced (image (c) in Figure 5).

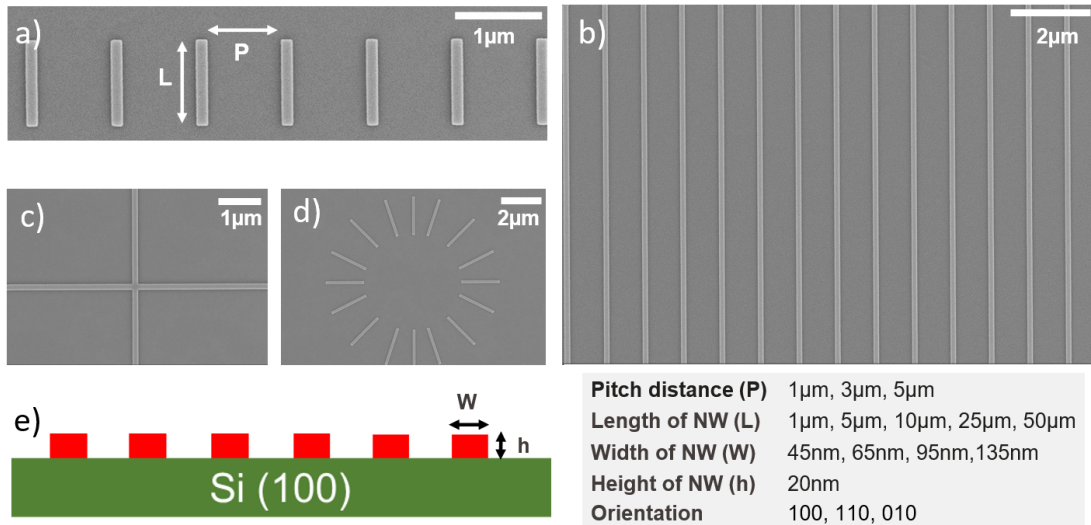| Pitch distance (P) | 1µm, 3µm, 5µm |
Length of NW (L)	1µm, 5µm, 10µm, 25µm, 50µm
Width of NW (W)	45nm, 65nm, 95nm,135nm
Height of NW (h)	20nm
Orientation	100, 110, 010

Figure 5: *(a) and (b) SEM images of amorphous NWs with different lenght, acquired before annealing. (c) NWs cross shaped network. Evaporation allows to grow NWs networks. This is useful for quantum computing applications since it provides a simple way to link different quantum dots. (d) Amorphous NWs in a circular arrangement. Evaporation gives also the possibility to grown NWs with peculiar arrangements. (e) Schematic cross section of the deposited NWs.*

Once the fabrication process was completed, SEM images of the nanowires (Figure 6) were used to assess the real size (width) of the nanowires. These images, taken before annealing, confirmed the real nanowires sizes to be in accordance with the theoretical ones, with an error below 10%.
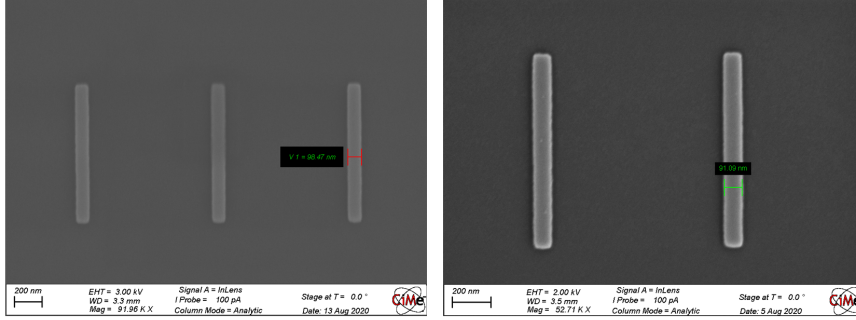

Figure 6: *SEM images: through SEM images we measured the real sizes (width) of the nanowires in order to compare them with the predicted ones. They confirmed the real nanowires sizes to be in accordance with the theoretical ones, with an error below 10%.*

All these operations were carried out at room temperature, thus the nanowires were amorphous after the deposition. They were crystallized, using the solid phase epitaxy approach, through rapid thermal annealing (RTP JETFIRST 200) at different temperatures for different times. The performed series are:

- 500°C for 10 sec

- 650°C for 10, 60, 120 sec

- 800°C for 10 sec

Before starting the analysis on the crystallized nanowires, a power study was performed on amorphous samples in order to assure that the laser exposition (532 nm wavelength) did not affect the nanowires crystal structure. The amorphous nanowires were exposed to different laser powers, from very low power values (19 uW) to the values we used for the nanowires analysis in section 5 (2,5 mW and 1,25 mW), to study the effects on the crystal structure. In the power range 19 uW – 490 uW, the more the power was reduced the more the measurement times were increased in order to obtain an intelligible spectrum (otherwise, for such low powers it was difficult to observe and analyze the Raman spectra). The power study clearly showed that the laser (532 nm) did not crystallize the amorphous samples. All the spectra (Figure 7) exhibited the same trend suggesting that the laser, in the power range we investigated, did not significantly affected the crystal structure. The only noticeable difference is the ratio between the broad Germanium peak and

12

the noise fluctuations. Indeed, spectra taken at lower laser powers showed higher background noise due to the longer time taken for the acquisition.
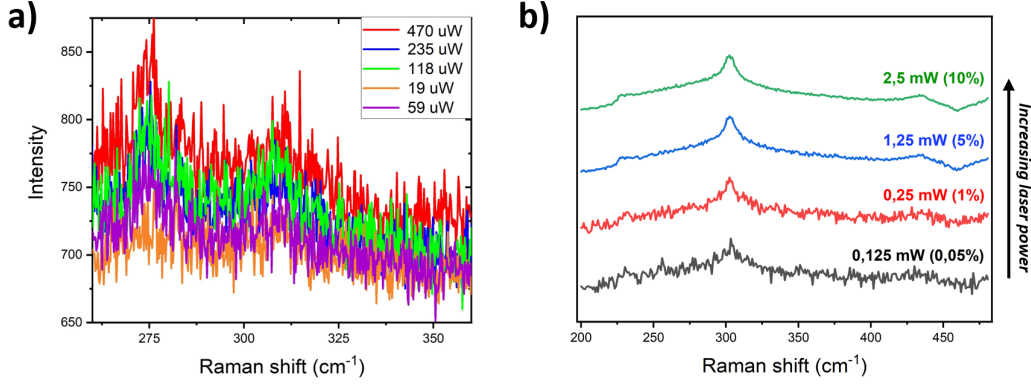

Figure 7: *Power study Raman spectra: (a) Comparison of low laser powers spectra, acquired with the material science department Raman spectrometer. (b) Comparison of high laser powers spectra, acquired with the Renishaw Raman spectrometer in physics department. In both cases no substantial changes were detected suggesting that the laser, in the power range we investigated, did not significantly affected the NWs crystal structure.*
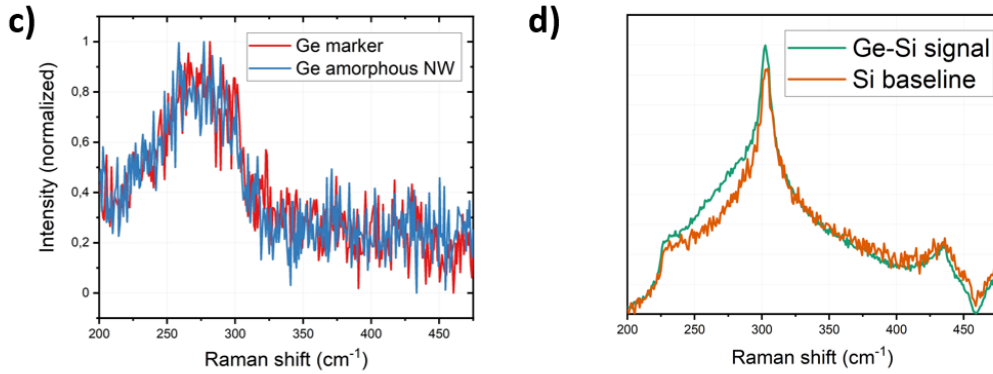

Figure 8: *Power study Raman spectra: (c) comparison of two spectra, one acquired from an amorphous Ge marker (red line), the other acquired from the amorphous NWs (blue line). The two spectra overlap confirming that the laser exposition did not have a significant effect on the NWs crystal structure. (d) The spectrum in blue in fig.c represents the signal coming exclusively from Ge. It has been obtained by subtracting the signal coming from the Si substrate (orange line) from the signal coming from the amorphous NWs (green line) which includes both the contributes of Ge and Si substrate.*

13

In Figure 8 are displayed two Raman spectra, acquired using a laser power of 1,25 mW. The two spectra overlap confirming that the laser exposition did not have a significant effect on the nanowires crystal structure.

After that, Raman spectra acquisition process was optimized investigating which laser intensity and baseline subtraction method gave the best spectra.
The firsts Raman measurements showed non-reproducible spectra with very broad and asymmetric peaks. These features were just artifacts coming from an underestimation of the importance of the signal to noise ratio. Once a proper laser power has been adopted (we used 1,25mW and 2,5mW for the Raman analysis) these artifacts disappeared and the Raman measurements returned reproducible results. Once we gathered which laser powers gave the best results, we focused on the baseline subtraction method. Baseline subtraction is fundamental for nanowires Raman analysis since, because of the nanowires size, the spectrometer always detects a strong signal from the Si substrate. Different baseline subtraction methods were tested in the initial phase of this project. The most effective turned out to be the following (Figure 9): for every measurement, a Raman spectrum taken from the pure Silicon substrate was properly rescaled and subtracted from the nanowires spectrum, revealing the signal coming exclusively from Germanium.
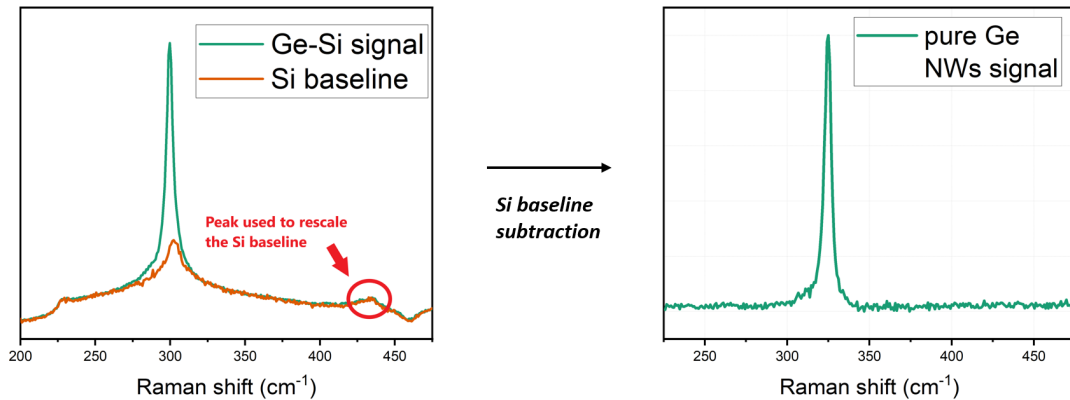

Figure 9: *Baseline subtraction method: in order to subtract the Si baseline (background signal coming from the Si substrate) and reveal the signal coming exclusively from Ge NWs, a Si Raman spectrum acquired from the pure Si substrate was properly rescaled and subtracted from the NWs Raman spectra (including both Ge NWs and Si substrate contributions). In the pictures it is shown a spectrum acquired from the Ge NWs (green), before and after the subtraction of the signal coming from the Si substrate (orange). Baseline subtraction is fundamental with NWs Raman analysis since the spectrometer always detects a strong signal from the Si substrate.*

In order to rescale the Silicon spectrum different peaks could have been used. The most convenient to exploit was the Silicon peak around 430 cm^{-1}: it is was not significantly affected by annealing temperature changes and it did not show any sub-

14

stantial variation in the spectra taken from the Si substrate and from Ge nanowires since it is located far from Ge-Ge peak, around 300 cm^{-1}.

This method allowed us to obtain reproducible results, subtracting the baseline without manipulating the data.

Finally, the crystalline Germanium nanowires were characterized by Raman spectroscopy in order to analyze the crystal quality and assess the presence of defects, strain and intermixing occurring at the interface. In addition, scanning electron microscopy was used to investigate nanowires surface morphology, before and after the rapid thermal annealing. Transmission electron microscopy was than exploited to assess the presence of defects and analyze nanowires crystal structure. In the end, a chemical characterization through EDX was carried out to investigate the presence of Oxygen at the interface between Si and Ge.

5 Results and Conclusions

In the following section will be presented the results and the conclusions of our analysis of the crystallized nanowires. The nanowires were studied through Raman spectroscopy, scanning electron microscopy and transmission electron microscopy. In the end, a chemical characterization through EDX was carried out.

5.1 Variations in crystal quality as a function of NWs morphology and orientation

We analyzed the nanowires through Raman spectroscopy in order to evaluate (in a qualitative fashion) the crystal quality, the crystal phase, strain presence and
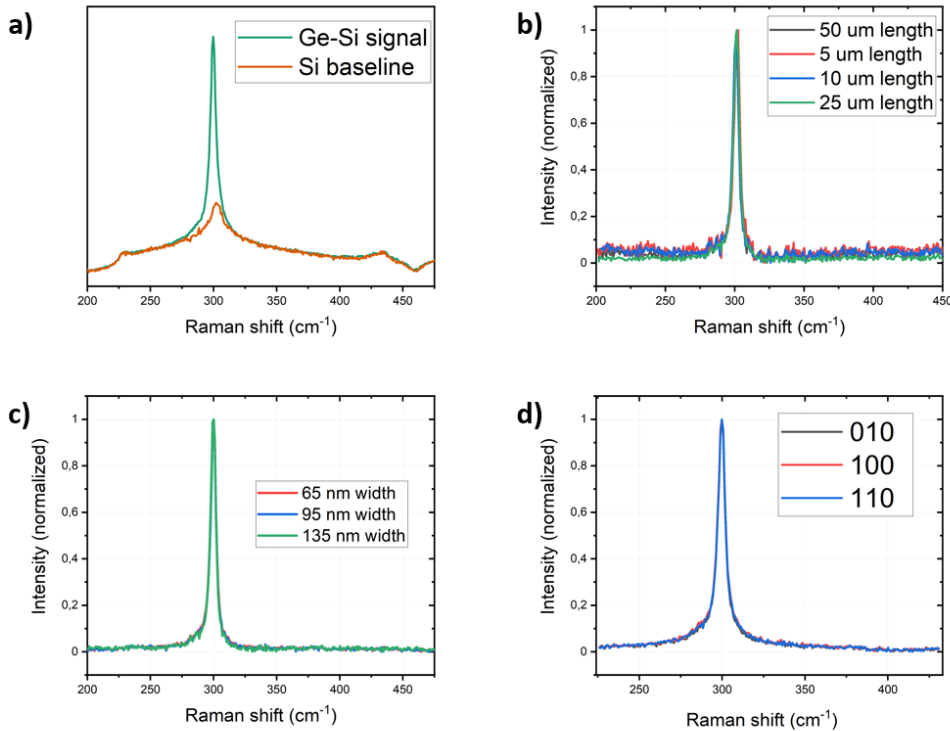

Figure 10: *Raman analysis of samples annealed at 650°C for 120 sec: (a) Superposition of the signal coming from the NWs, which includes both the contributes from Ge and from the Si substrate (green line) and signal coming from the pure Si substrate (orange line). (a) Comparison of Raman spectra acquired from NWs with varying length. (c) Comparison of Raman spectra acquired from NWs with varying width. (d) Comparison of Raman spectra acquired from NWs with varying orientation. The spectra perfectly overlapped showing no significant changes with varying length, width and orientation.*

possible intermixing occurring at the interface between Ge and Si. Indeed FWHM (full width at half maximum) of Raman peaks is related to crystal quality: low FWHM values correspond to good crystal quality, a perfect crystalline Germanium Raman peak is characterized by a FWHM of 3.2 - 3.5 cm^{-1}. On the other hand, broad symmetric peaks are associated with amorphous phase while sharp peaks with a crystalline structure, allowing to gain a qualitative analysis of crystal phase. For each of the five performed annealing series (different annealing times and temperatures, see list Figure 4.2) we compared Raman spectra of nanowires with different length, width and orientation (as shown in the images of Figure 10) in order to investigate how they responded to the annealing procedure and we looked for some trends related to the varying parameters. Similar results were observed for all the different series. The spectra perfectly overlapped showing no significant changes with varying length and orientation. In contrast with our expectations, the spectra did not show any change even with varying width. We expected thinner nanowires to relax more easily crystal defects, with a consequent effect on Raman spectra. When Germanium is epitaxially grown on Silicon, as explained in section 1, it accumulates energy in the form of strain at the interface, which could lead to the spontaneous formation of misfit dislocations. Usually when a material is heated up, dislocations tend to move towards grains boundaries in bulk materials. In case of nanostructures, due to the small size, dislocations tend to move to the side walls, where they can relax more easily.

These results could be due to the presence of native oxide (confirmed by EDX analysis, see Figure 14) on the Silicon substrate which prevented the formation of an epitaxial relation between the substrate and the deposited nanowires [21, 22]. In case an oxide is present, Germanium does not undergo any kind of strain because of the lack of an epitaxial relation with Silicon. This implies that no strain relaxation mechanism occurs, leading to the absence of dislocations at the interfaces.

During nanowires fabrication Silicon Dioxide has been removed by wet etching through a solution containing 1% of Hydrofluoric acid, however Ge has not been deposited immediately after this procedure. Indeed, the evaporator Leybold optics Lab 600H used for deposition is not equipped with a load lock that allows to quickly reach the vacuum level (around 10^6 Pa) required for the process. It features only one chamber which requires more than one hour of pumping in order to achieve the desired pressure. We suspect it is during this time interval that Silicon may have spontaneously formed an oxide layer reacting with Oxygen in the air before it was pumped out.

5.2 Variation in crystal quality as a function of annealing temperature and time

In order to understand the effect of different annealing temperatures on nanowires crystal quality, we performed various annealing series using different temperatures.
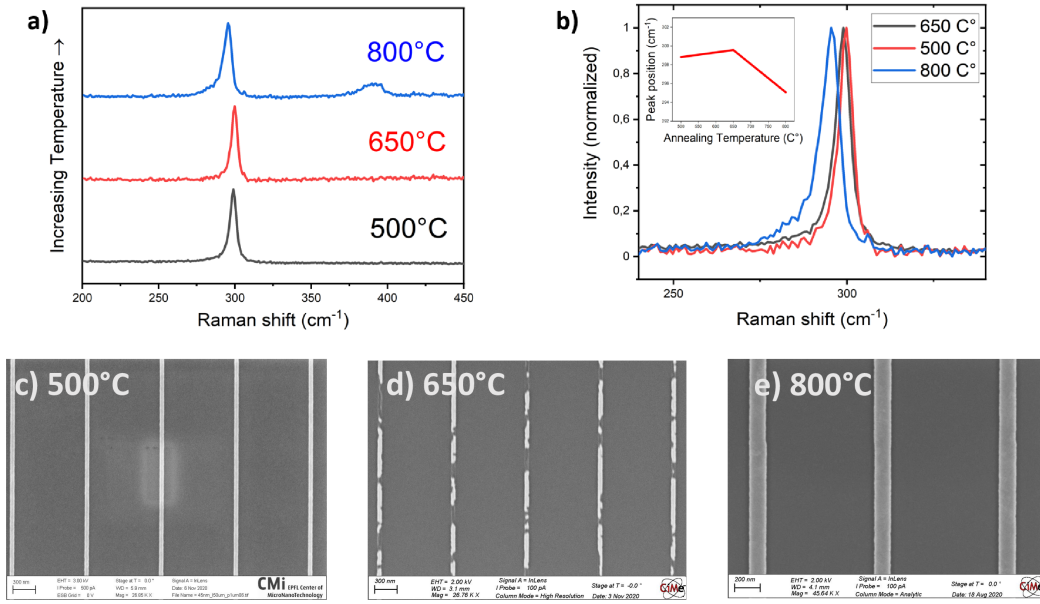
Figure 11: *Effects of different annealing temperatures: (a) Comparison of samples annealed at different temperatures: 800°C, 650°C, 500°C (10 seconds). Samples annealed at 800 °C displayed a Si-Ge peak around 400 cm^{-1} associated with the presence of intermixing. (b) Effects of different annealing temperatures on peak position. Ge Peak position trend is reported in the top left corner, numerical data are reported in Table 5.2. A peak shift towards lower Raman shifts for samples annealed at 800°C confirmed the detrimental effect of intermixing. (c,d,e) SEM images of samples annealed at different temperatures: 800°C, 650°C, 500°C. Samples annealed at 650°C (10,60,120 sec) have been damaged: NWs structures presented various cracks and holes. (More images in Appendix A)*

Raman spectra of samples annealed at 800 °C for 10 seconds displayed a Si-Ge peak around 400 cm^{-1} (Figure 11, (a)) associated with the presence of intermixing at the interface [23], not observed for nanowires annealed at 500°C and 650°C.
Raman spectra also revealed a peak shift towards lower Raman shifts for samples annealed at 800°C (Figure 11, (b)), confirming the detrimental effect of intermixing. Indeed, this shift could be a direct consequence of the activation of Ge phonon modes with k different from zero, caused by the defective nature of intermixing. Light (laser used in Raman spectroscopy) cannot provide the necessary momentum to activate them but impurities or defects in the crystal structures can scatter phonons, triggering these modes (Figure 2 for more details).
Figure 11 shows the comparison of three spectra acquired from samples annealed for 10 seconds at different temperatures: 500°C, 650°C, 800°C. Intermixing affected crystal quality, indeed FWHM values, extracted through Lorentian fit of the peaks, exhibited a significant increment for samples annealed at 800°C, as it shown in Table 5.2, associated with a degradation of crystal quality with respect to 500°C

and 650°C samples. Perfect crystalline Germanium Raman peak is characterized by a FWHM of 3.2 - 3.5 cm^{-1}, while our samples from 800°C annealing series featured FWHM with values above 5 cm^{-1}.

Table 1: *Effects of different annealing temperatures*

Temperature (°C)	Peak Position (cm^{-1})	FWHM (cm^{-1})
500	298,82097 ± 0,02624	4,8216 ± 0,06057
650	299,57359 ± 0,0304	4,18872 ± 0,08802
800	295,07767 ± 0,07525	5,63509 ± 0

SEM images of the nanowires surfaces revealed further effects of the annealing process. Indeed, samples annealed at 650°C (10,60,120 sec) have been damaged, while samples annealed at 500°C and 800°C have not. As shown in Figure 11, nanowires structure presented various cracks and holes. This could be due to the following reason: since Ge and Si feature a different thermal expansion coefficient their lattice parameters will increase with different rates under annealing. The more the annealing temperature increases the more the strain affecting Ge nanowires, due to lattice mismatch, will increase. However, at some point Si interdiffusion will occur at the interface between the nanowires and the substrate, making Ge adapt to Si behaviour. Therefore we suppose that samples annealed at 650°C cracked because of the excessive strain induced by high temperatures, while samples annealed at 800°C did not crack, despite the higher temperatures in play, thanks to the effect of intermixing which has reduced the strain experienced by the nanowires.

In order to investigate the effect of longer annealing times we compared the spectra acquired from the three different annealing series performed at 650°C.
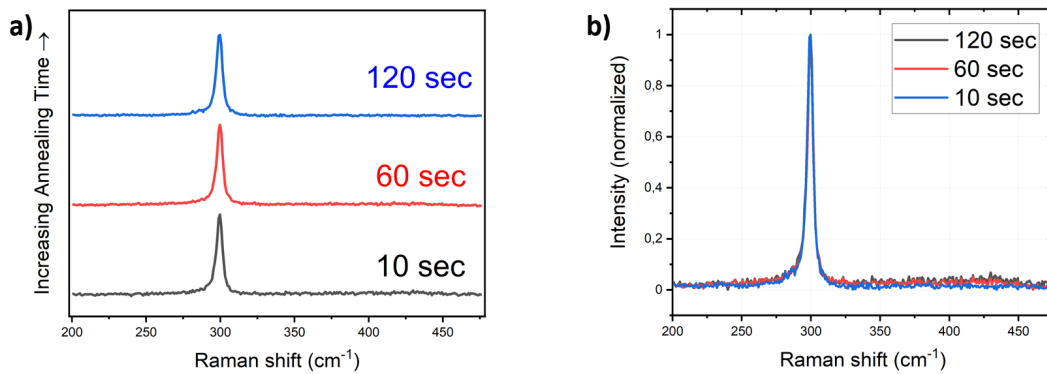

Figure 12: *Effects of different annealing times: (a) comparison of three spectra acquired from samples annealed at 650°C for different times: 10 sec, 60 sec, 120 sec. (b) The three spectra perfectly overlap, showing that no substantial changes have been detected by Raman spectroscopy.*

Figure 12 shows that no substantial changes have been detected by Raman spectroscopy for the sets of nanowires annealed for 10, 60, 120 seconds.

5.3 Crystal structure analysis and chemical characterization

TEM analysis were conducted on the sample annealed at 500°C for 10 sec, the one not damaged by the thermal annealing and not affected by intermixing, to investigate the crystal structure after annealing.
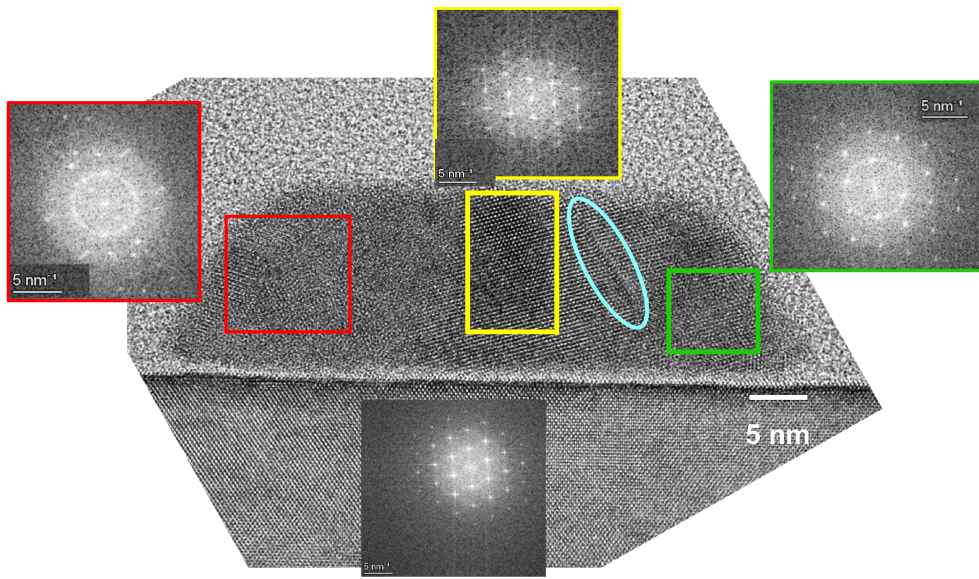

Figure 13: *TEM image of the Si-Ge interface. In the coloured boxes are reported the FFT pattern related to different sample locations. Different FFT patterns from different locations revealed that the NWs presented a polycrystalline structure. A microtwin is clearly visible in the TEM image (light blue oval). Both polycrystalline structure and microtwins formation could be caused the presence of an oxyde layer between the NWs and the Si substrate.*

We expected to have monocrystalline Germanium since it was suppose to epitaxially grow on a monocrystalline Silicon substrate. However, TEM image in Figure 13 shows different crystal orientations at different locations, as it can be gathered from the FFT pattern, reveling that the nanowires presented a polycrystalline structure. This can be explained considering the presence of the oxide layer between Silicon and deposited Germanium. The absence of an epitaxial relation with the substrate made the nanowires crystallize randomly, leading the formation of a polycrystalline structure.

TEM images also assessed the presence of microtwins in the crystal structure (Figure 13). These crystal defects have been observed in previous studies [22, 24] in

the presence of interfacial oxygen. This is due to the fact that oxide has the effect to suppress the growth process. In case of a nonuniform oxygen distribution at the interface this effect leads to an inhomogeneous growth rate which produces an atomically distorted growth front. In this conditions microtwins will form, more easily where higher Oxygen concentrations are present, as reported by Ichiro Mizushima et al. [22].

The existence of crystal defects in the nanowires structure could be the cause of the shoulder present on the left of the Ge peaks (see images of Figure 10). In addition it could also explain why, even for a sample not affected by intermixing, Raman spectra displayed a small red shift and a slight peak broadening with respect to the ideal values. Indeed, Germanium peak positions and FWHM (Table 5.2) did not respectively reach the values of 300 cm^{-1} and 3.2 - 3.5 cm^{-1}, characteristic of perfect monocrystalline defect free Ge peak.
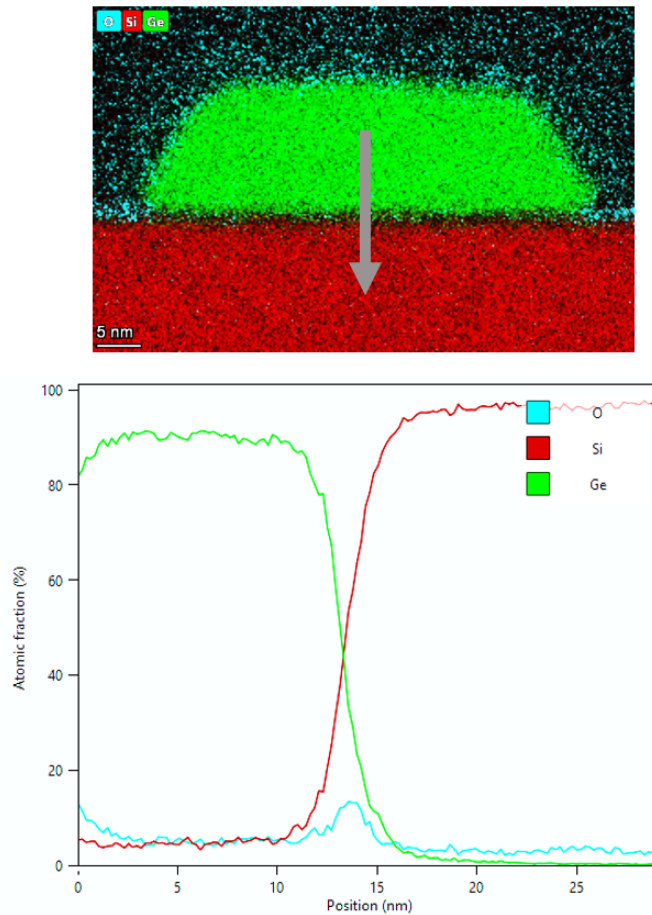

Figure 14: *EDX analysis: chemical characterization of the NWs substrate interface. The graph shows the chemical element concentration trends along the grey arrow direction. EDX confirmed that an oxyde layer spontaneously formed on the Silicon surface, as attested by the small Oxygen peak displayed.*

Energy Dispersive X-Ray (EDX) chemical characterization was carried out to assess the presence of Oxygen between the deposited nanowires and the Si substrate. Figure 14 confirmed that an oxyde layer spontaneously formed on the Silicon surface, preventing the formation of an epitaxial relation between Ge and Si. The graph displaying the chemical elements concentrations clearly shows this result. A small Oxygen peak rises between Si and Ge confirming the presence of Oxygen at the interface.

5.4 Conclusions

We successfully fabricated Ge NWs with different width, pitch, length and orientation through evaporation and lift-off. This method also provided a simple way for growing NWs networks and it leaves open the possibility of mass production. Both these features are fundamental for quantum computing applications.
We have also studied the crystallization behaviour of the NWs, in relation to rapid thermal annealing: samples annealed at 650°C cracked because of the excessive high temperatures induced stress experienced by the crystal structure, while samples annealed at 800°C showed the presence of intermixing at the interface, which we suppose helped to prevent the cracking.
In conclusion, the best annealing parameters, among those ones we investigated, turned out to be 500°C - 10 seconds since NWs spectra exhibited sharp peaks (absence of amorphous phase), relatively low values of FWHM (indicating a good crystal quality) and did not show any damage due to excessive annealing temperatures.

Our next goal is improving the fabrication process in order to avoid the formation of an oxyde layer and deposit the amorphous Germanium directly on Silicon, establishing an epitaxial relation between the substrate and the NWs. This will hopefully allow to obtain defects free monocrystalline Ge NWs with good crystal quality (and enhanced hole mobility due to induced strain) which will be used as core of Ge-Si core-shell quantum dots.

References

[1] Håkon Ikaros T. Hauge et al. "Single-Crystalline Hexagonal Silicon–Germanium". In: *Nano Letters* 17.1 (2017). PMID: 28001429, pp. 85–90. DOI: 10.1021/acs.nanolett.6b03488. eprint: https://doi.org/10.1021/acs.nanolett.6b03488. URL: https://doi.org/10.1021/acs.nanolett.6b03488.

[2] Li Z. Pei and Zheng Y. Cai. "A Review on Germanium Nanowires". In: *Recent Patents on Nanotechnology* 6.1 (2012), pp. 44–59. ISSN: 1872-2105/2212-4020. DOI: 10.2174/187221012798109291. URL: http://www.eurekaselect.com/node/94811/article.

[3] Dunwei Wang et al. "Surface Chemistry and Electrical Properties of Germanium Nanowires". In: *Journal of the American Chemical Society* 126.37 (2004). PMID: 15366907, pp. 11602–11611. DOI: 10.1021/ja047435x. eprint: https://doi.org/10.1021/ja047435x. URL: https://doi.org/10.1021/ja047435x.

[4] B. Yu et al. "One-dimensional Germanium Nanowires for Future Electronics". In: *Journal of Cluster Science* 17 (Dec. 2006), pp. 579–597. DOI: 10.1007/s10876-006-0081-x.

[5] Amrit De and Craig E Pryor. "Electronic structure and optical properties of Si, Ge and diamond in the lonsdaleite phase". In: *Journal of physics. Condensed matter : an Institute of Physics journal* 26.4 (2014). DOI: doi:10.1088/0953-8984/26/4/045801.

[6] Xavier Cartoixà et al. "Optical Emission in Hexagonal SiGe Nanowires". In: *Nano Letters* 17.8 (2017). PMID: 28654293, pp. 4753–4758. DOI: 10.1021/acs.nanolett.7b01441. eprint: https://doi.org/10.1021/acs.nanolett.7b01441. URL: https://doi.org/10.1021/acs.nanolett.7b01441.

[7] Saurabh Dixit and A. Shukla. "Optical properties of lonsdaleite silicon nanowires: A promising material for optoelectronic applications". In: *Journal of Applied Physics* 123 (June 2018), p. 224301. DOI: 10.1063/1.5025856.

[8] Claudia Fasolato et al. "Crystalline, Phononic, and Electronic Properties of Heterostructured Polytypic Ge Nanowires by Raman Spectroscopy". In: *Nano Letters* 18.11 (2018). PMID: 30185053, pp. 7075–7084. DOI: 10.1021/acs.nanolett.8b03073. eprint: https://doi.org/10.1021/acs.nanolett.8b03073. URL: https://doi.org/10.1021/acs.nanolett.8b03073.

[9] Wei Lu et al. "One-dimensional hole gas in germaniumsilicon nanowire heterostructures". In: *Proceedings of The National Academy of Sciences - PNAS* (Jan. 2005). DOI: doi:10.1073/pnas.0504581102.

[10] Hannes Watzinger et al. "A germanium hole spin qubit". In: *Nature Communications* 9 (Sept. 2018). DOI: 10.1038/s41467-018-06418-4.

[11] "Surface-enhanced Raman spectroscopy - Wikipedia". In: *Wikipedia, consulted on november 2020, last update October 2020* (). URL: https://en.wikipedia.org/wiki/Surface-enhanced_Raman_spectroscopy.

[12] Naoki Fukata et al. "Doping and Raman Characterization of Boron and Phosphorus Atoms in Germanium Nanowires". In: *ACS Nano* 4.7 (2010). PMID: 20565120, pp. 3807–3816. DOI: 10.1021/nn100734e. eprint: https://doi.org/10.1021/nn100734e. URL: https://doi.org/10.1021/nn100734e.

[13] Cruz-Irisson M. Wang-Chen C. Alfaro-Calderón P. "Theory of Raman Scattering by Phonons in Germanium Nanostructures". In: *Nanoscale Res Lett* 3.55 (2008). DOI: https://doi.org/10.1007/s11671-007-9114-0.

[14] H. Peelaers, Bart Partoens, and F. Peeters. "Phonons in Ge nanowires". In: *Applied Physics Letters* 95 (Oct. 2009), pp. 122110–122110. DOI: 10.1063/1.3236526.

[15] Kunimitsu Uchinokura, Tomoyuki Sekine, and Etsuyuki Matsuura. "Raman scattering by silicon". In: *Solid State Communications* 11.1 (1972), pp. 47–49. ISSN: 0038-1098. DOI: https://doi.org/10.1016/0038-1098(72)91127-1. URL: http://www.sciencedirect.com/science/article/pii/0038109872911271.

[16] Chris Finlayson et al. "Electrical and Raman Characterization of Silicon and Germanium-filled Microstructed Optical Fibers". In: *Applied Physics Letters* 90 (Mar. 2007). DOI: 10.1063/1.2713755.

[17] D. Rouchon et al. "Germanium content and strain in Si1xGex alloys characterized by Raman spectroscopy". In: *Journal of Crystal Growth* 392 (Apr. 2014), pp. 66–73. DOI: 10.1016/j.jcrysgro.2014.01.019.

[18] Katherine Macarthur. "The Use of Annular Dark-Field Scanning Transmission Electron Microscopy for Quantitative Characterisation". In: *Johnson Matthey Technol. Rev.* 60 (Mar. 2016), p. 117. DOI: 10.1595/205651316x691186.

[19] "Thin films – Center of MicroNanotechnology CMi - EPFL". In: *EPFL CMi website, consulted on november 2020* (). URL: https://www.epfl.ch/research/facilities/cmi/equipment/thin-films/.

[20] "Lift-off (microtechnology)". In: *Wikipedia, consulted on november 2020, last update July 2020* (). URL: https://en.wikipedia.org/wiki/Lift-off_(microtechnology).

[21] Martin Steglich et al. "Heteroepitaxial Ge-on-Si by DC magnetron sputtering". In: *AIP Advances* 3 (July 2013). DOI: 10.1063/1.4813841.

[22] Ichiro Mizushima et al. "Oxide-Mediated Solid Phase Epitaxy (OMSPE) of Silicon: A New Low-Temperature Epitaxy Technique Using Intentionally Grown Native Oxide". In: *Japanese Journal of Applied Physics* 39 (Apr. 2000), pp. 2147–2150. DOI: 10.1143/JJAP.39.2147.

[23] Xiaolong Zhang, Wipakorn Jevasuwan, and Naoki Fukata. "Interfacial inter-mixing of Ge/Si core–shell nanowires by thermal annealing". In: *Nanoscale* 12 (Jan. 2020). DOI: 10.1039/C9NR09938G.

[24] I. Mizushima H. Kuwano T. Hamasaki T. Yoshii M. Kashiwagi. "Effect of interfacial oxide on solid-phase epitaxy of Si films deposited on Si substrates". In: *Journal of Applied Physics 63, 1065* (1988). DOI: https://doi.org/10.1063/1.5022078.

A Appendix

In this section I will present some additional figures which I did not add to the Lab Report in order to keep it short.
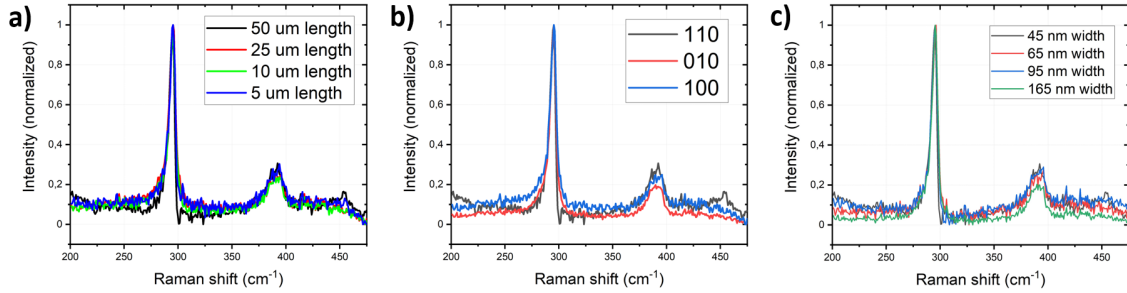

Figure 15: *Raman analysis of samples annealed at 800°C for 10 sec: (a) Comparison of Raman spectra acquired from NWs with varying length. (b) Comparison of Raman spectra acquired from NWs with varying orientation. (c) Comparison of Raman spectra acquired from NWs with varying width. The spectra perfectly overlapped showing no significant changes with varying length, width and orientation. The spectra displayed a Si-Ge peak around 400 cm⁻¹ associated with the presence of intermixing at the interface, not detected for samples annealed at 650°C and 500°C.*
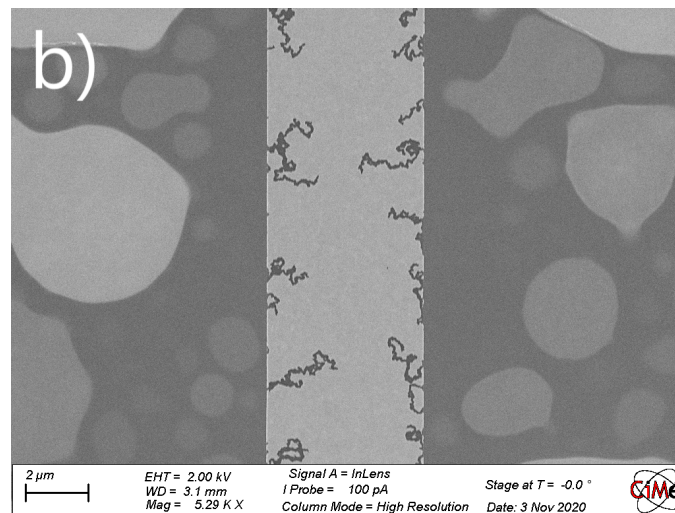

Figure 16: *SEM image: high magnification SEM image that allows to observe in details the damages caused by high temperature annealing. Samples annealed at 650°C cracked because of the excessive strain induced by high temperatures*